Available online at www.worldscientificnews.com

World Scientific News

An International Scientific Journal

WSN 192 (2024) 22-44 EISSN 2392-2192

Numerical Analysis and Simulations of Thermo-Fluidic Flow of Johnson-Segalman Fluid in a Circular Pipe

Rafiu Olalekan Kuku[1], **Nurudeen Adekunle Raji**[2] and **Gbeminiyi Sobamowo**[3]

Department of Mechanical Engineering, Faculty of Engineering, Lagos State University, Epe Campus, Lagos, Nigeria

[1-3]E-mail address: rafiu.kuku@lasu.edu.ng , nurudeen.raji@lasu.edu.ng , gsobamowo@unilag.edu.ng

ABSTRACT

This current research presents a mathematical model and analysis of flow and heat transfer in a Johnson-Segalman fluid in a circular pipe. A numerical solution to the governing equations is found by applying a finite difference technique. The effects of relevant parameters, such as the relaxation time parameter, viscosity parameter, and Brinkman number, on the fluid velocity and temperature distributions of the pipe flow are examined using the numerical solutions that were produced. The results demonstrate that as the relaxation time parameter and Brinkman number increase, so do the fluid velocity and temperature. Additionally, it was shown that the relaxation time parameter rises as fluid velocity increases but falls as fluid temperature rises. The impact of relaxation factors on the velocity distribution has insignificant effect on the flow process when the viscosity parameter gets closer to and larger than unity. The findings of this investigation are generally consistent with those of the earlier study as documented in the literature.

***Keywords*:** Heat transfer, Pipe flow, Johnson-Segalman fluid, Analytical solutions, finite difference method

(Received 21 February 2024; Accepted 18 March 2024; Date of Publication 20 March 2024)

1. INTRODUCTION

The increasing awareness of and use of numerous industrially significant fluids that defy Newton's law of viscosity has sparked interest in the study of fluids under a variety of circumstances in recent years. Non-Newtonian fluids include things like blood, synovial fluid, honey and tomato sauce, slurries, pastes, gels, molten plastics, and lubricants incorporating polymer additives [1, 2]. Furthermore, non-Newtonian and non-Navier-Stokes mathematical models have been developed in order to predict the flow of complex fluids used in industrial processing, such as paints, melts, and polymer solutions. These models were developed in response to the limitations and inadequacies of the classical Navier-Stokes equations in describing the rheological behaviors of these fluids under different conditions. In the previous few decades, a variety of new models have been presented for non-Newtonian fluids, including upper-convected Maxwell fluid, Oldroyd-B fluid, second-order, third-order, and fourth-order fluids. The viscosity of these non-Newtonian fluid types is constant. In actuality, however, the viscosity of a non-Newtonian fluid changes with the rate of shear or the fluid's prior kinematic history at a given temperature and pressure [3]. It follows that not all non-Newtonian behaviors can be adequately described and predicted by a single constitutive connection. As a result, several rate-type fluid models were created. A viscoelastic fluid model was created in addition to many other rate-type fluids to account for non-affine deformations in the Johnson–Segalman (J–S) fluid model, which was created to characterize the flow behaviors of non-Newtonian fluids. The model is flexible and it considers the memory and elastic properties found in most biological and polymeric fluids. Among the various fluids of the rate type models, the model has received special prominence recently since it incorporates special cases like the Oldroyd-B fluid, the classical Newtonian fluid, the Navier-Stokes fluid, and the Maxwell fluid. For a specific range of material parameters, the J-S fluid, in contrast to most other fluid models, permits a non-monotone relationship between the shear stress and velocity gradient in simple shear flows, leading to solutions with discontinuous velocity gradients for planar and cylindrical Poiseuille flow. The "spurt" phenomena, which describes a significant increase in volume followed by a slight increase in driving, has been successfully explained by the model pressure gradient.

Numerous studies have been conducted to describe non-Newtonian fluid behaviors using the fluid model because of the fluid model's generic nature and significance in the study of flow behaviors of non-Newtonian fluids [6–20]. In these earlier works, many methods have been employed to solve the developed non-linear models. The argument over the past few decades has focused on the loss of convergence of numerical iterative algorithms for solving the flow of viscoelastic fluids at moderate values of the Deborah number, even if numerical approaches were used in some of the investigations. Furthermore, Howell [19] noted that the Weissenberg number—a physical parameter—increases with the difficulty of numerically simulating viscoelastic fluid movement. In particular, when the Weissenberg number exceeds a critical point, the iterative nonlinear solver becomes intractable. In order to approximate the solution to the heat transfer in pipe flow of Johnson-Segalman fluid, Hayat et al. [20] employed HAM.

The approach solves differential equations without the need for discretization, linearization, approximation, linearization restrictive assumptions or perturbations, complicated derivative expansion, or symbolic derivative computing. Furthermore, it may be applied to nonlinear problems without any small or big parameters, and it can be a useful tool for managing the convergence of approximation series and modifying the convergence zone as

needed [21]. Finding a specific auxiliary parameter that would fulfill the boundary condition in the second place, however, could add to the computational burden of coming up with a workable solution. This disadvantage is not limited to HAM, determining the parameters that will meet the second boundary condition also needed additional computing time and expense when using other approximate analytical methods like HPM, DTM, ADM, and VIM. Furthermore, the majority of approximation techniques only produce reliable forecasts for moderate nonlinearities; strong nonlinear models do not yield reliable predictions from them. Additionally, HAM required intricate mathematical analysis that produced an analytical expression with many terms, and when it is often used, it occasionally produces inaccurate findings [22, 23].

In real life, engineers and designers find it difficult to employ approximative analytical solutions containing a lot of terminology. In addition, it is a laborious task that requires strong mathematical abilities. Simple yet correct expressions are inevitably needed in order to resolve the non-linear formula. Also, a numerical method such as finite different method represents an efficient way of obtaining temperature profile for the heat transfer processes. In the numerical method, the choice of finer grids which requires high computing capability can remove approximation errors to larger extent. Therefore, in this research, a mathematical model and analysis of heat transfer in a Johnson-Segalman fluid pipe flow is presented using finite difference method. The result obtained by the method (for solving the problem under investigation) was compared with the previous studies and a very good agreement was established. The effects of relevant parameters, such as the relaxation time parameter, viscosity parameter, and Brinkman number, on the fluid velocity and temperature distributions of the pipe flow are examined.

2. MODEL FORMULATION

Consider a steady state pipe flow of incompressible Johnson-Segalman fluid which is induced by pressure gradient in the z-direction (axis of flow) in a circular pipe of radius r_o shown in Fig. 1.

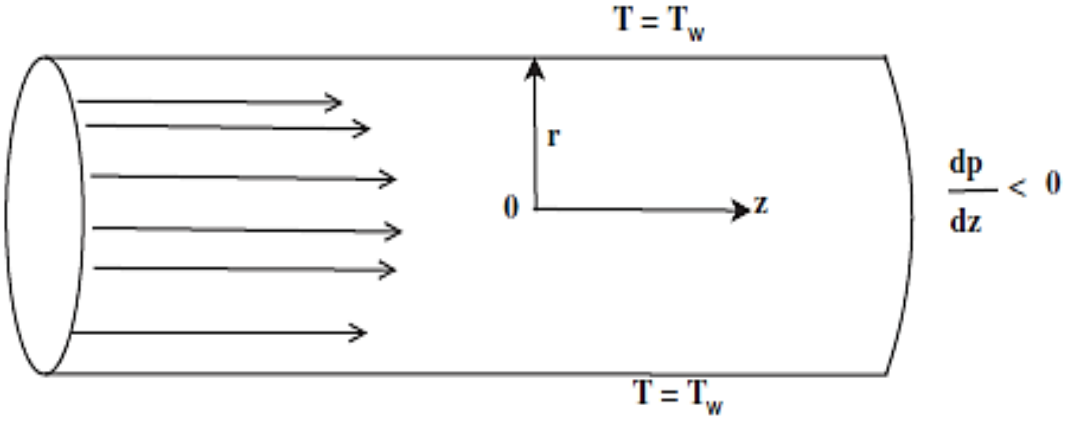

Fig. 1. Schematic of the problem

As the fluid is incompressible, it can undergo only isochoric motions. Therefore, with an appropriate choice of the kernel function and the time constants, the governing equations are

Continuity equation

$$\nabla.\bar{u} = 0 \tag{1}$$

Momentum equation

$$\rho\left(\frac{\partial \bar{u}}{\partial t} + \bar{u}\nabla\bar{u}\right) = \nabla.\sigma \tag{2}$$

Energy equation

$$\sigma\,.\,\Upsilon + k\nabla^2 T = \rho c_p \frac{\partial T}{\partial t} \tag{3}$$

where

$$\sigma = -p\mathrm{I} + \tau \tag{4}$$

$$\tau = 2\mu D + S \tag{5}$$

$$S + \xi\left\{\frac{\partial S}{\partial t} + v\nabla S + S(W - aD) + (W - aD)^t S\right\} = 2\eta D \tag{7}$$

$$D = \frac{1}{2}\left(\Upsilon + \Upsilon^t\right) \qquad W = \frac{1}{2}\left(\Upsilon - \Upsilon^t\right) \tag{8}$$

where (t) represents the matrix transpose. It is be noted that this model includes the Oldroyd-B fluid model for $a=1$. When $a=1$, $\mu=0$ the Johnson–Segalman fluid model reduces to the Maxwell fluid model, when $\xi = 0$ the model reduces to the classical Navier–Stokes fluid model and when $\xi=0$, $\mu=0$ the model reduces to the classical Newtonian fluid model. It should be noted that the bracketed term on the left-hand side of Eq. (7) is an objective time derivative.

The governing equations of motion in cylindrical coordinates give

$$\frac{\partial p}{\partial r} = \frac{1}{r}\frac{d}{dr}\left(rS_{rr}\right) - \frac{S_{\theta\theta}}{r} \tag{9a}$$

$$\frac{\partial p}{\partial \theta} = 0 \tag{9b}$$

$$\frac{\partial p}{\partial z} = \frac{1}{r}\frac{d}{dr}\left(rS_{rz}\right) + \frac{\mu}{r}\frac{d}{dr}\left(r\frac{d\bar{u}}{dr}\right) \tag{9c}$$

$$\left(\frac{d^2T}{dr^2}+\frac{1}{r}\frac{dT}{dr}\right)\left\{1+\xi\left(1-a^2\right)\left(\frac{d\bar{u}}{dr}\right)^2\right\}+\frac{\mu}{k}\xi\left(1-a^2\right)\left(\frac{d\bar{u}}{dr}\right)^4+\frac{(\eta+\mu)}{k}\left(\frac{d\bar{u}}{dr}\right)^2=0 \tag{10}$$

where

$$S_{rr}=\frac{-\xi(1-a)\eta\left(\frac{d\bar{u}}{dr}\right)^2}{1+\xi(1-a^2)\left(\frac{d\bar{u}}{dr}\right)^2} \tag{11a}$$

$$S_{rz}=\frac{\eta\frac{d\bar{u}}{dr}}{1+\xi(1-a^2)\left(\frac{d\bar{u}}{dr}\right)^2} \tag{11b}$$

$$S_{\theta\theta}=0 \tag{11c}$$

It should be noted that while Eq. (9c) and (10) can be used to find the velocity and temperature distributions in the pipe, Eq. (9a) can be adopted to find the pressure distribution in the pipe. However, our major focus in this work is to find velocity and temperature distributions in the pipe.

From Eq. (9c) and (11a), we have

$$\frac{\partial p}{\partial z}=\frac{1}{r}\frac{d}{dr}\left\{r\left[\frac{(\eta+\mu)\frac{d\bar{u}}{dr}+\xi\mu(1-a^2)\left(\frac{d\bar{u}}{dr}\right)^3}{1+\xi(1-a^2)\left(\frac{d\bar{u}}{dr}\right)^2}\right]\right\} \tag{12}$$

The boundary condition are given as

$$r=0,\quad \frac{du}{dr}=0,\quad \frac{dT}{dr}=0$$
$$r=r_o,\quad u=0,\quad T=T_w \tag{13}$$

where T_w is the wall temperature.

On non-dimensionalizing Eqs.(10), (12) and (13) using the following dimensionless quantities, where T_m is the wall temperature.

$$R=\frac{r}{r_o},\quad u=\frac{\mu}{\left(\frac{\partial p}{\partial z}\right)r_o^2}\bar{u},\quad \lambda=\frac{\xi\left(1-a^2\right)\left(\frac{\partial p}{\partial z}\right)^2}{\mu^2}r_o^2 \tag{14}$$

$$\alpha=\left(1+\frac{\eta}{\mu}\right),\quad \theta=\frac{T-T_w}{T_m-T_w},\quad B_r=\frac{R^4\left(\frac{\partial p}{\partial z}\right)^2}{kT_w\mu}$$

We have

$$\frac{d}{dR}\left\{R\left[\frac{\alpha\frac{du}{dR}+\lambda\left(\frac{du}{dR}\right)^3}{1+\lambda\left(\frac{du}{dR}\right)^2}\right]\right\}-R=0 \tag{15}$$

$$R\frac{d^2\theta}{dR^2}+\frac{1}{R}\frac{d\theta}{dR}+R\lambda\frac{d^2\theta}{dR^2}\left(\frac{du}{dR}\right)^2+\lambda\frac{d\theta}{dR}\left(\frac{du}{dR}\right)^2+R\alpha B_r\left(\frac{du}{dR}\right)^2+R\lambda B_r\left(\frac{du}{dR}\right)^4=0 \tag{16}$$

Eq. (15) can be further simplify after integration of both side w.r.t R as

$$2\lambda\left(\frac{du}{dR}\right)^3+2\alpha\frac{du}{dR}-R\lambda\left(\frac{du}{dR}\right)^2-R=0 \tag{17}$$

$$R\frac{d^2\theta}{dR^2}+\frac{1}{R}\frac{d\theta}{dR}+R\lambda\frac{d^2\theta}{dR^2}\left(\frac{du}{dR}\right)^2+\lambda\frac{d\theta}{dR}\left(\frac{du}{dR}\right)^2+R\alpha B_r\left(\frac{du}{dR}\right)^2+R\lambda B_r\left(\frac{du}{dR}\right)^4=0 \tag{18}$$

The boundary conditions are given as

$$R=0,\quad \frac{du}{dR}=0,\quad \frac{d\theta}{dR}=0$$

$$R=1,\quad u=0,\quad \theta=0 \tag{19}$$

where T_w is the wall temperature.

3. NUMERICAL SOLUTIONS OF THE NONLINEAR THERMAL MODELS

The developed Eqs. (17) and (18) contain nonlinear models that are extremely challenging to precisely and analytically solve. Thus, we turned to the finite difference method (FDM), a numerical technique. The decision was reached because the finite difference approach, which has been used to the solution of several linear and non-linear differential equations in literature, can be utilized to solve differential equations involving one or more independent variables. An effective method of getting the temperature profile for the steady heat transfer processes is by the numerical solution of FDM. Any complex body can be solved with the FDM by segmenting the body into manageable domains. Choosing finer grids, which calls for a lot of processing power, can also eliminate approximation mistakes more thoroughly. The method of finite differences is comparatively more stable and more straightforward, accurate, and efficient. Therefore, the finite difference method is applied in this work.

The equivalent finite difference schemes for equations (17) and (18) are as follows:

$$2\lambda\left(\frac{u_{i+1}-u_{i-1}}{2\Delta R}\right)^3+2\alpha\left(\frac{u_{i+1}-u_{i-1}}{2\Delta R}\right)-i\Delta R\lambda\left(\frac{u_{i+1}-u_{i-1}}{2\Delta R}\right)^2-i\Delta R=0 \quad for \quad i=0,1,2,...N-1 \tag{20}$$

$$i\Delta R\left(\frac{\theta_{i+1}-2\theta_i+\theta_{i-1}}{(\Delta R)^2}\right)+\frac{1}{i\Delta R}\left(\frac{\theta_{i+1}-\theta_{i-1}}{2\Delta R}\right)+i\Delta R\lambda\left(\frac{\theta_{i+1}-2\theta_i+\theta_{i-1}}{(\Delta R)^2}\right)\left(\frac{u_{i+1}-u_{i-1}}{2\Delta R}\right)^2 \tag{21}$$

$$+\lambda\left(\frac{\theta_{i+1}-\theta_{i-1}}{2\Delta R}\right)\left(\frac{u_{i+1}-u_{i-1}}{2\Delta R}\right)^2+i\Delta R\alpha B_r\left(\frac{u_{i+1}-u_{i-1}}{2\Delta R}\right)^2+i\Delta R\lambda B_r\left(\frac{u_{i+1}-u_{i-1}}{2\Delta R}\right)^4=0 \quad for \quad i=0,1,2,...N-1$$

The boundary conditions are given as

$$i=0, \quad \left(\frac{u_1-u_{-1}}{2\Delta R}\right)=0 \quad \Rightarrow u_1=u_{-1}, \quad \left(\frac{\theta_1-\theta_{-1}}{2\Delta R}\right)=0 \quad \Rightarrow \theta_1=\theta_{-1} \tag{21}$$

$$i=N, \quad u_N=0, \quad \theta_N=0$$

4. RESULTS AND DISCUSSION

Figure 2-27 shows the numerical outcomes of the analytically determined solutions for the temperature and fluid velocity distributions in the half and full cylindrical coordinate systems. The charts illustrate how relevant parameters have an impact. The effects of the relaxation time parameter, λ, on the fluid velocity distribution are depicted in Figs. 2–7, while the velocity profile of the half cylindrical coordinate system of the effects of the viscosity parameter, α, on the fluid velocity distribution in the pipe is shown in Figs. 8–10. It should be noted that although the figures demonstrate that velocity increases with increasing λ and α, when α approaches unity and when it exceeds unity, as seen in Figs. 4 and 5, the effect of λ on the velocity distribution is not significant.

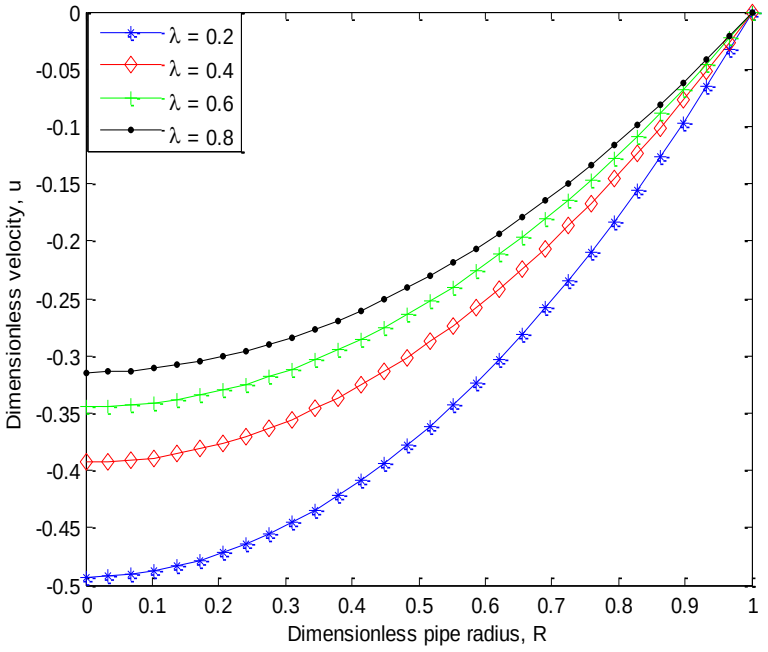

Fig. 2. Effect of λ on the fluid velocity, u when α =*0*

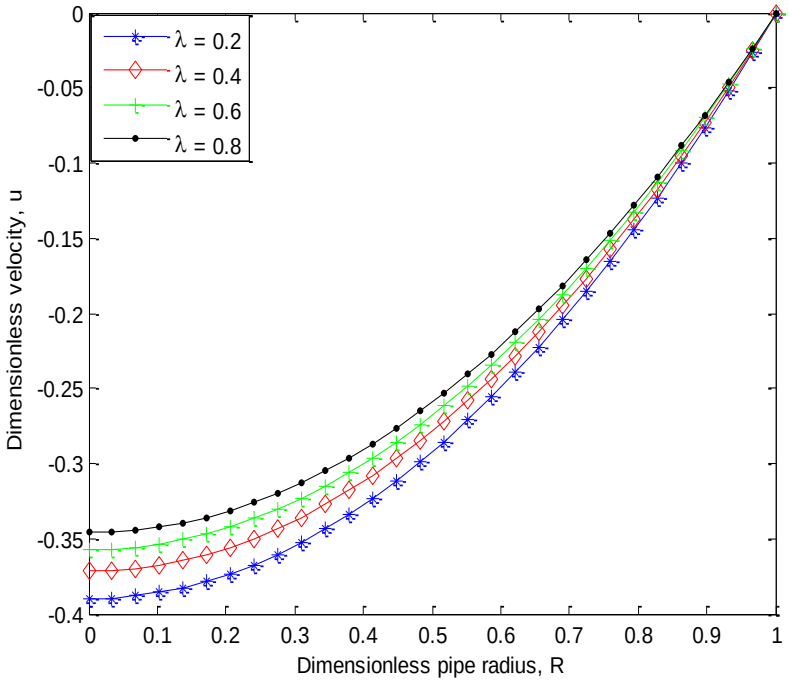

Fig. 3. Effect of λ on the fluid velocity, u when α =*0.5*

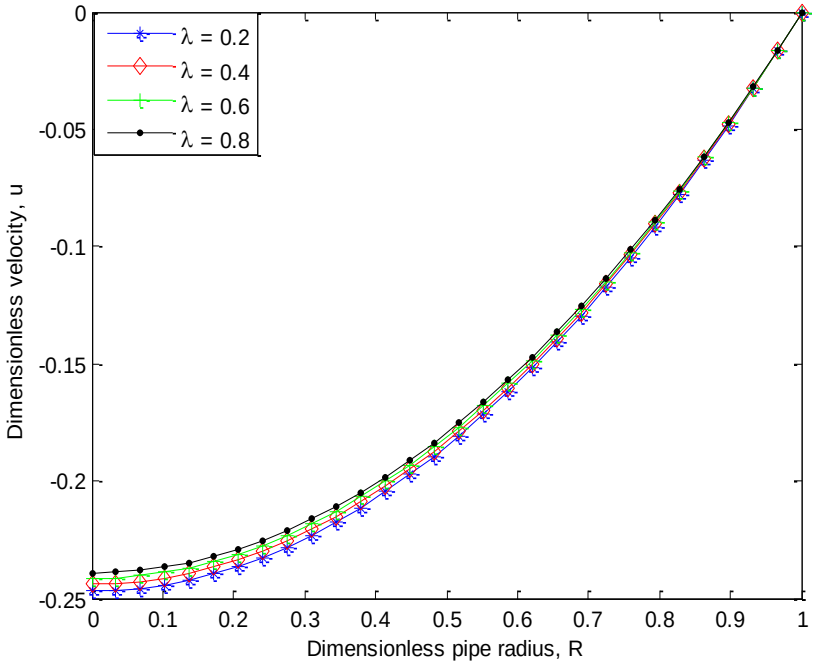

Fig. 4. Effect of λ on the fluid velocity, u when α *=0.75*

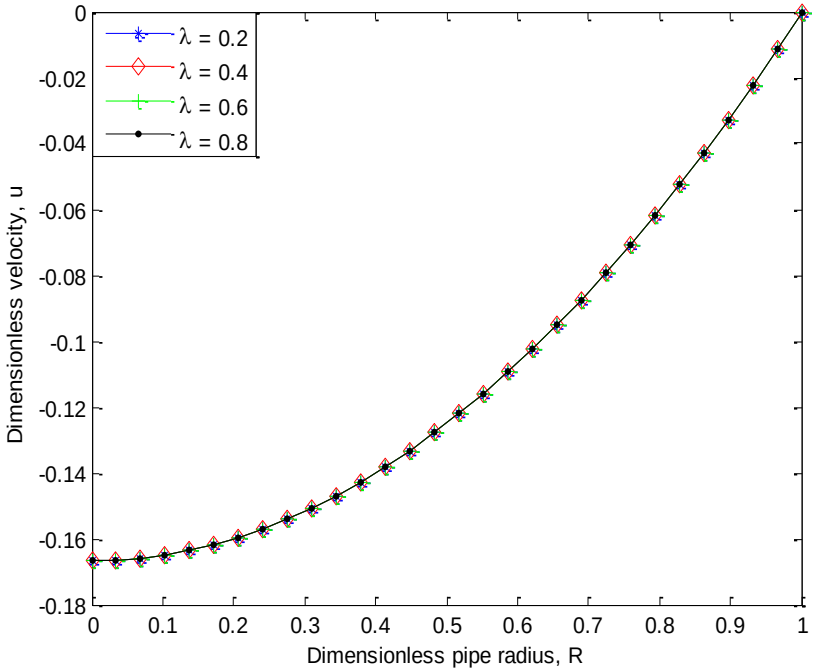

Fig. 5. Effect of λ on the fluid velocity, u when α *=1.0*

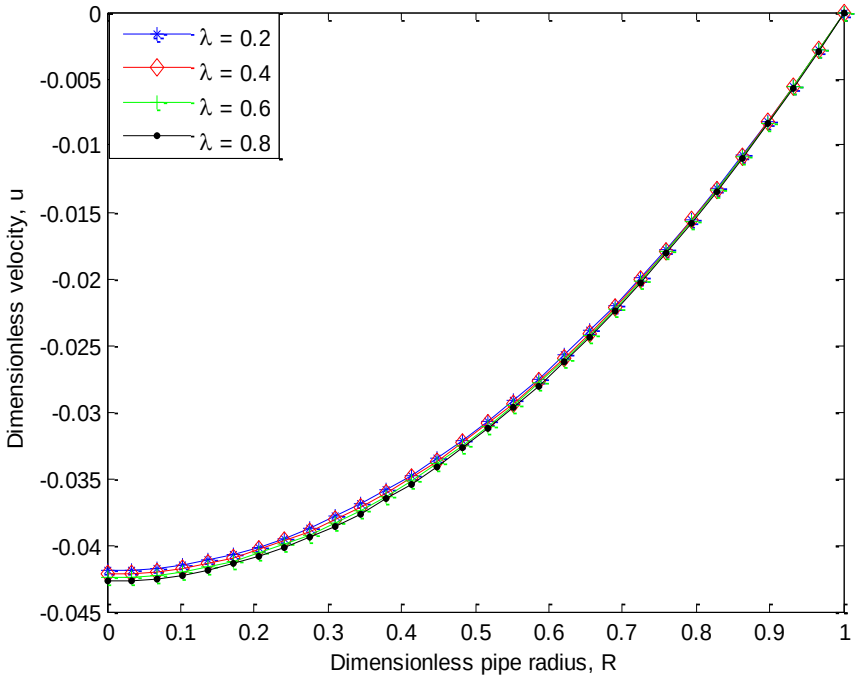

Fig. 6. Effect of λ on the fluid velocity, u when α =*2.0*

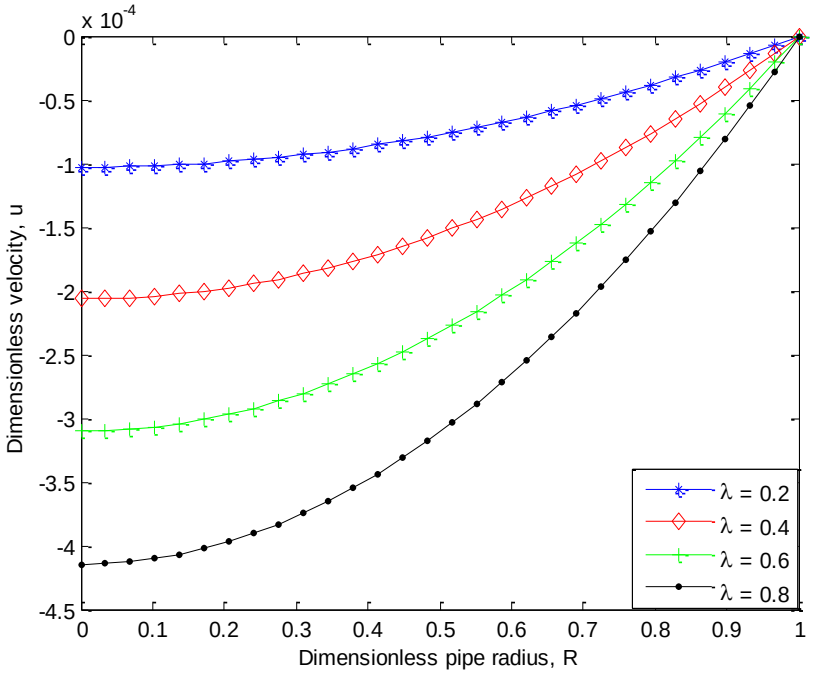

Fig. 7. Effect of λ on the fluid velocity, u when α =*3.0*

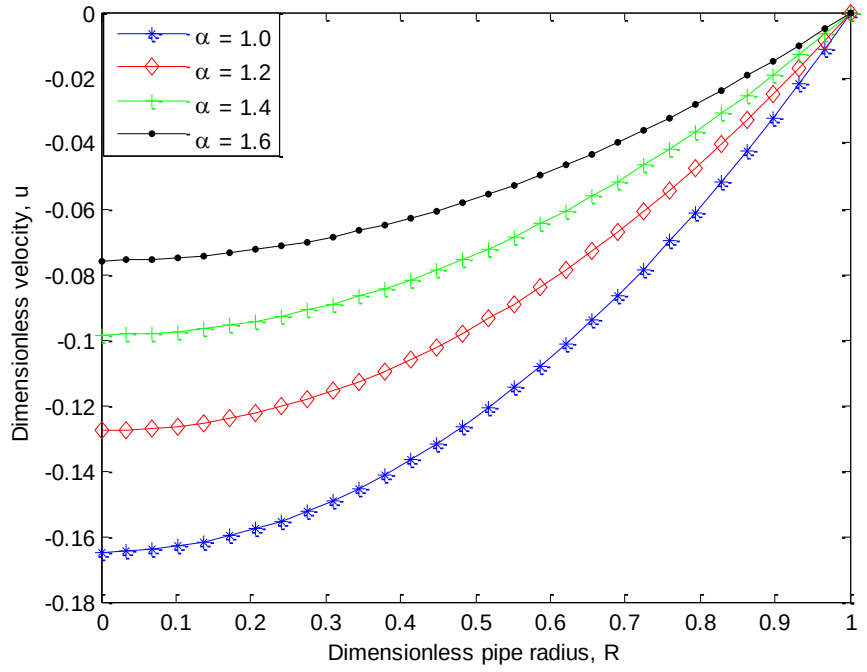

Fig. 8. Effect of α on the fluid velocity, u when λ =*0.5*

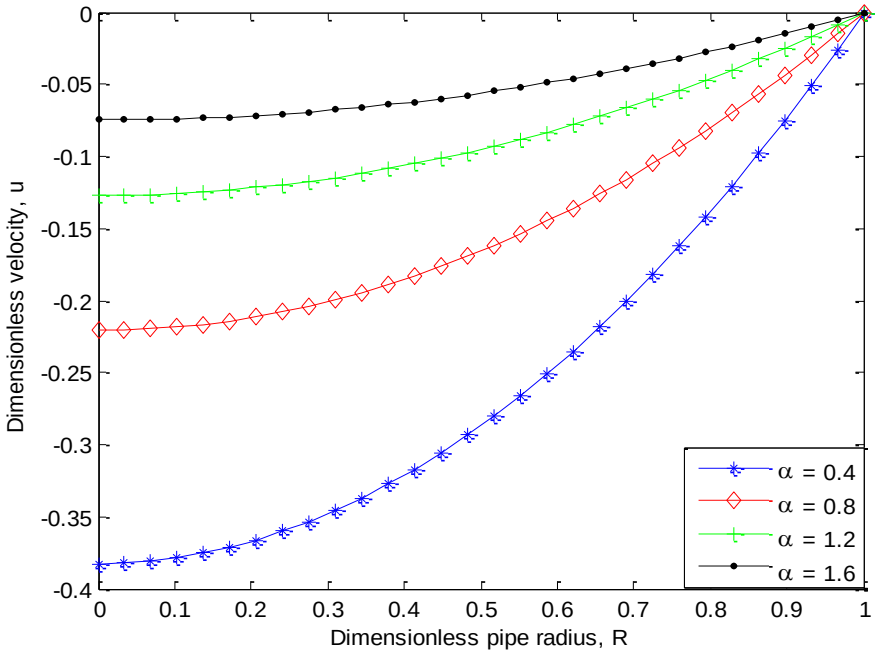

Fig. 9. Effect of α on the fluid velocity, u when λ =*0.75*

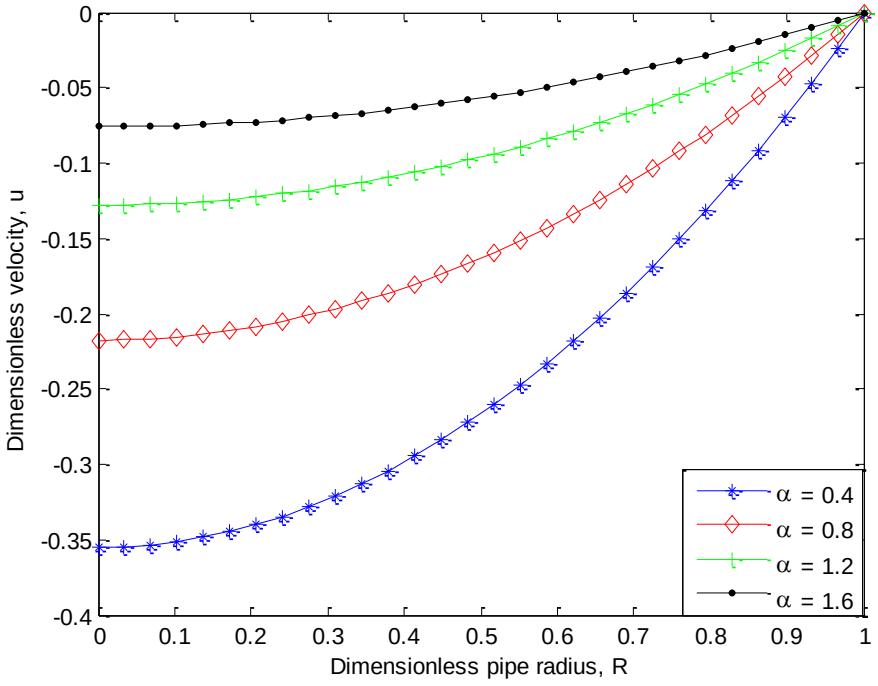

Fig. 10. Effect of α on the fluid velocity, u when λ *=1.0*

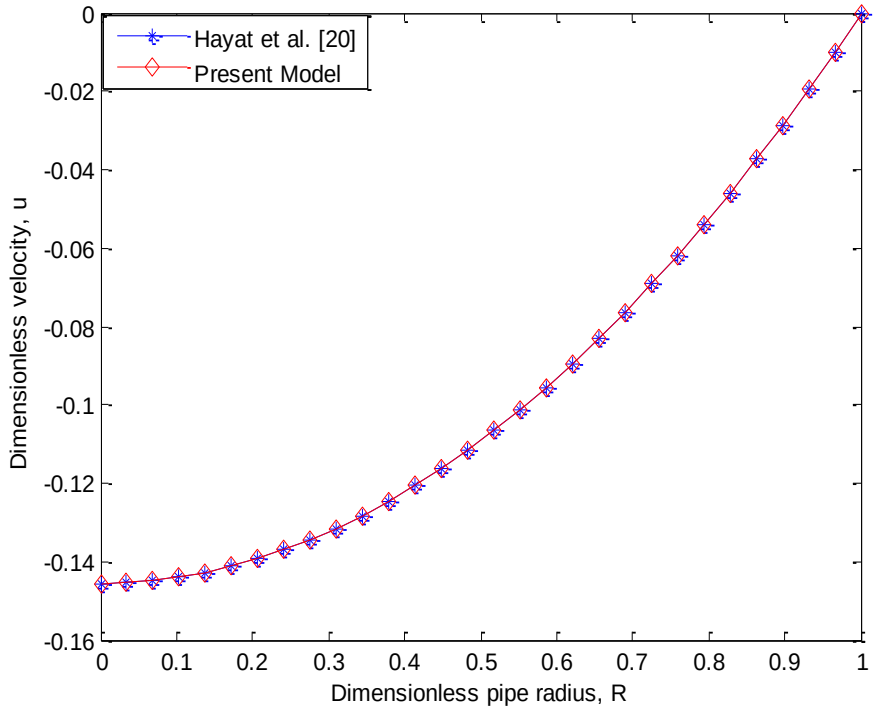

Fig. 11. Comparison of results

The findings of the analytical velocity field solution utilizing finite difference method of are compared with the HAM results provided by Hayat et al. [20] as illustrated in Fig. 11 in order to validate the numerical solutions in this work. The graph shows that the results reported in this publication were in good agreement with those of the earlier studies.

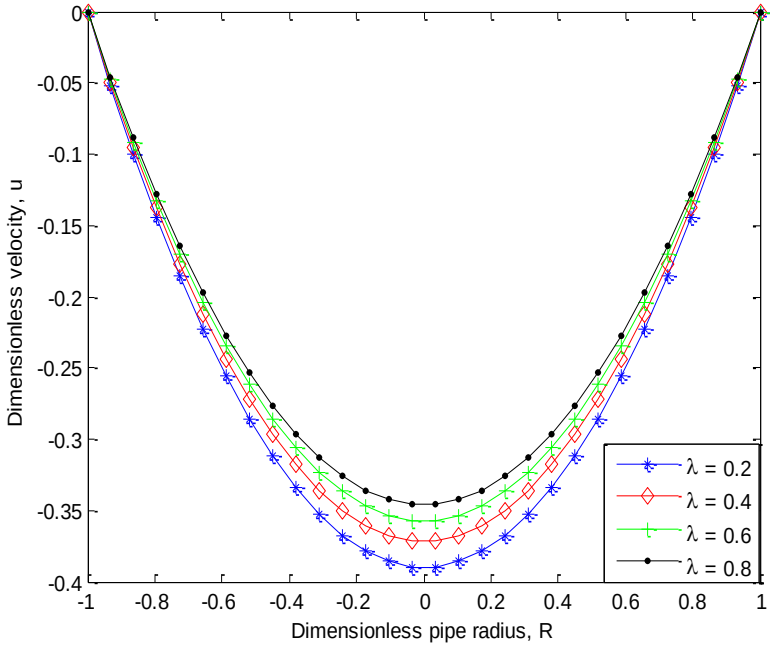

Fig. 12. Effect of λ on the fluid velocity, u when α =*0.5*

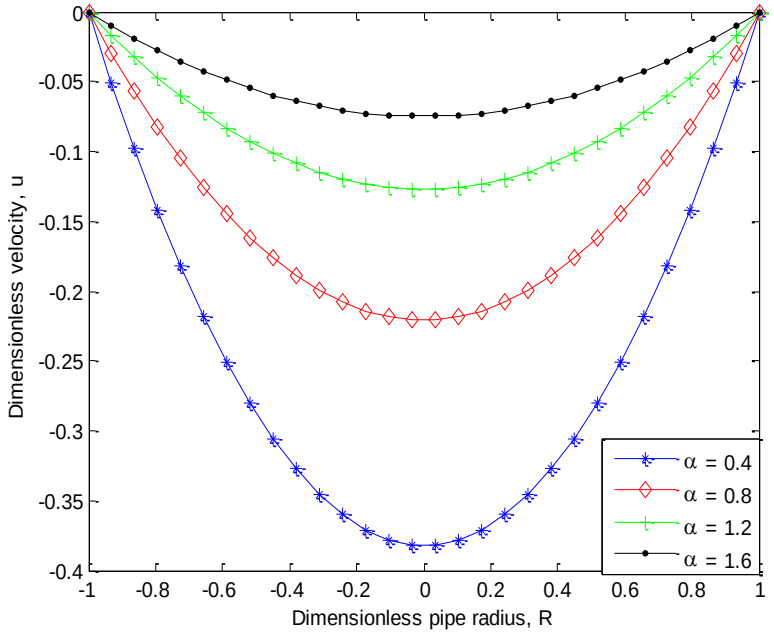

Fig. 13. Effect of α on the fluid velocity, u when λ =*0.5*

Fig. and Figs. 12 and 13 depict the velocity profile for the whole cylindrical coordinate system of the impacts of λ and α on the fluid velocity distribution in the pipe. Based on numerical data, it is evident that the pipe's center has the highest velocity, with values of λ and α that are more positive. The axial symmetry of the flow process and the fluid-structure interactions at the pipe walls, which result in the no-slip assumption at the walls, make this physically true. As a result, the fluid velocity increases toward the center of the pipe, drops near its walls, and reaches its maximum at its center.

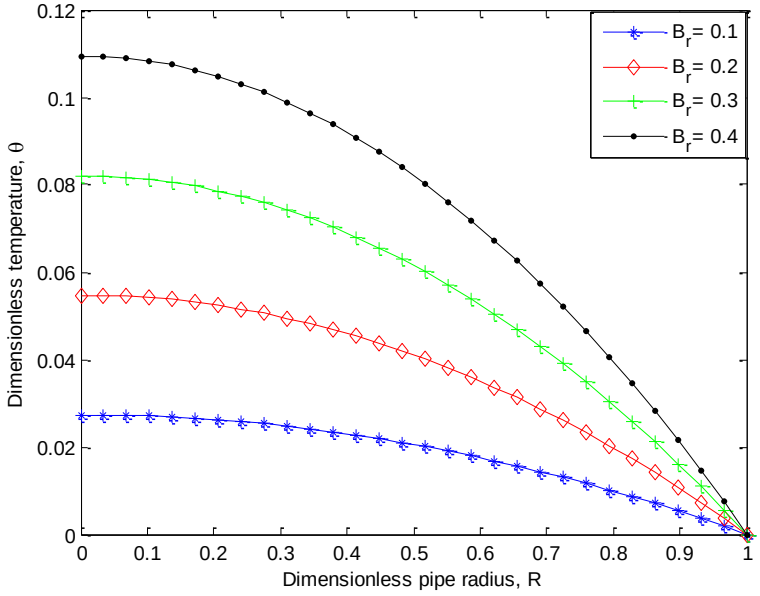

Fig. 14. Effect of B_r on the fluid temperature, λ *=0.5*, α *=0.5*

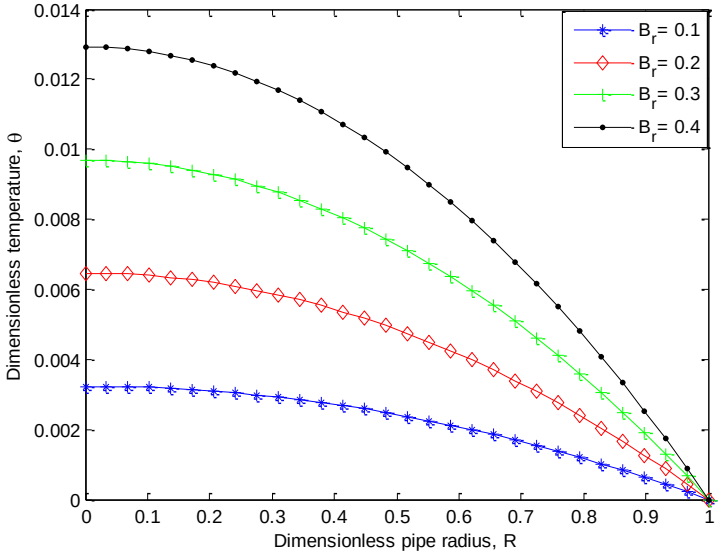

Fig. 15. Effect of B_r on the fluid temperature, λ *=0.5*, α *=1.5*

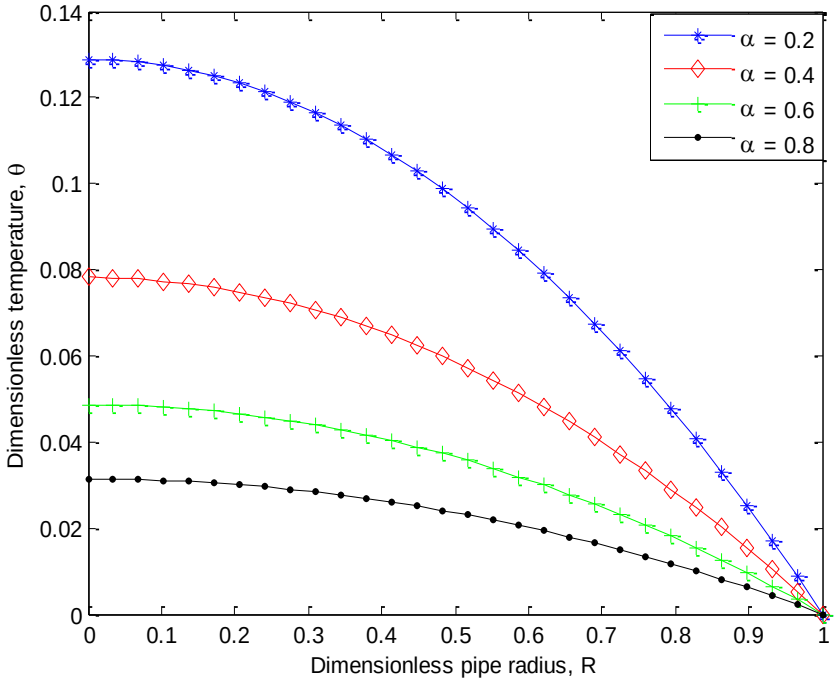

Fig. 16. Effect of α on the fluid temperature, B_r =0.2 λ =*0.5*

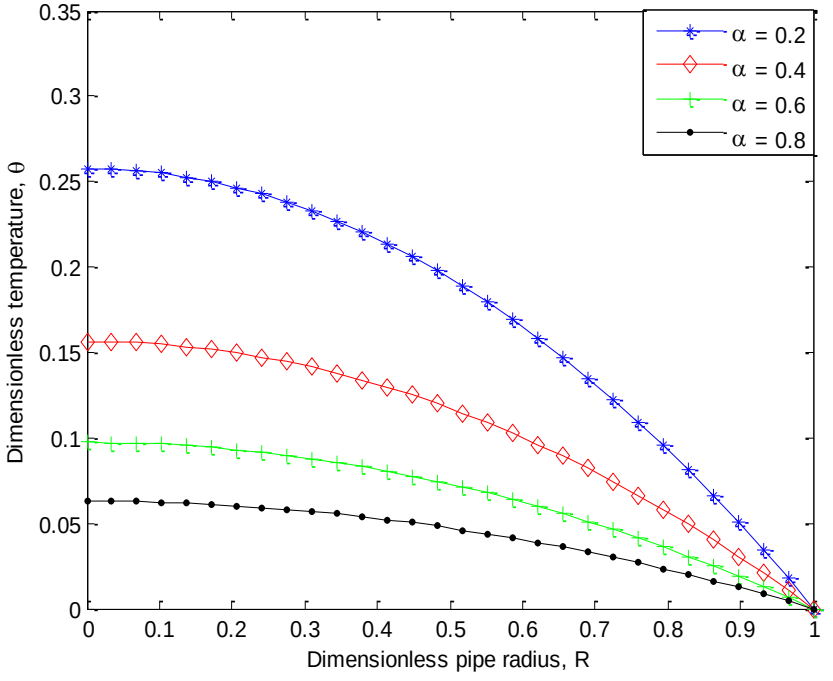

Fig. 17. Effect of α on fluid temperature, B_r =0.4 λ =*0.5*

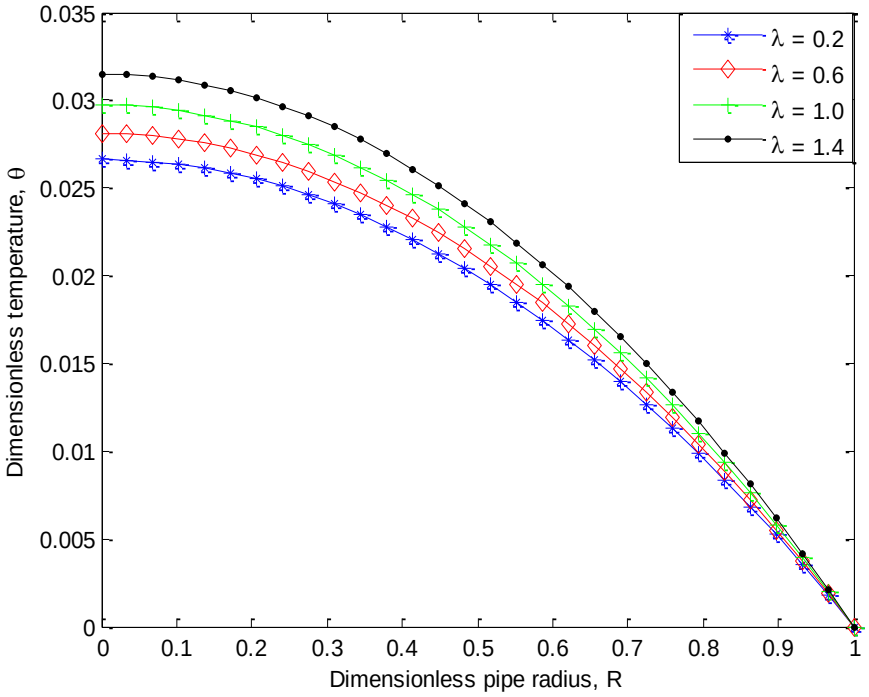

Fig. 18. Effect of λ on the fluid temperature, B_r =0.1 α =*0.5*,

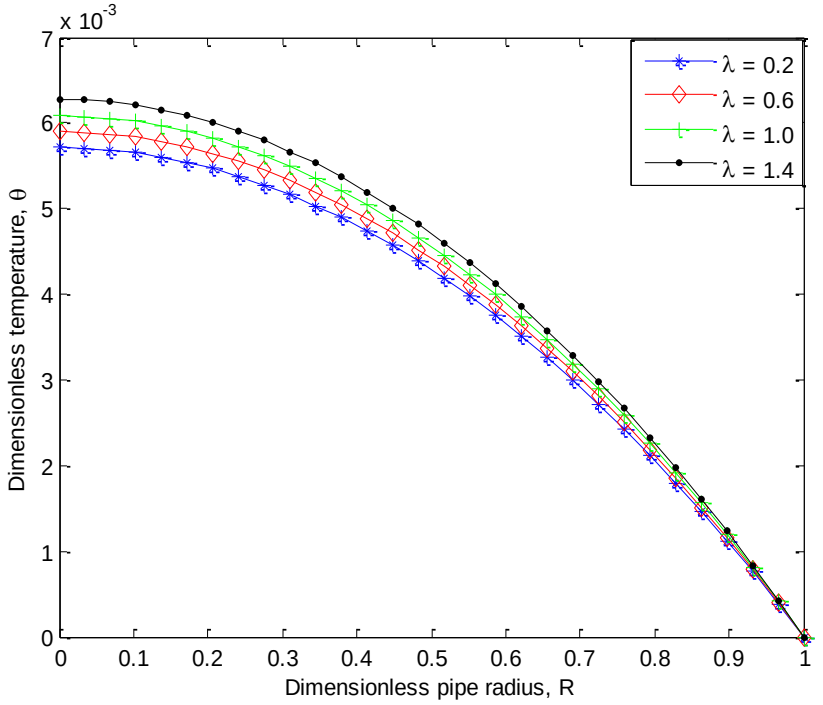

Fig. 19. Effect of λ on fluid temperature, B_r =0.1 α =*1.2*

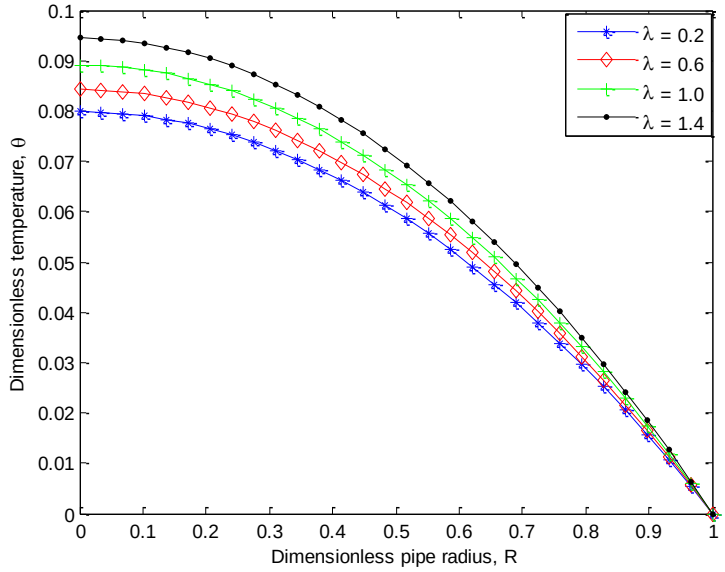

Fig. 20. Effect of λ on the fluid temperature, B_r =0.3, α *=0.5,*

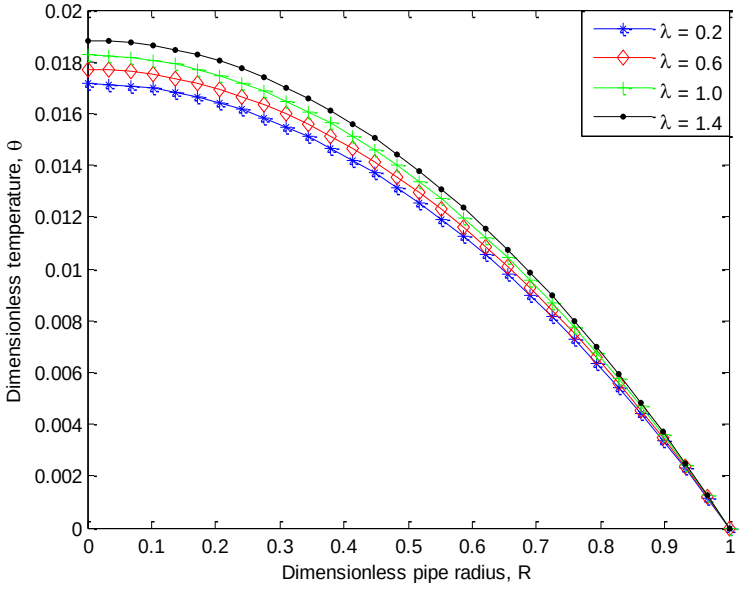

Fig. 21. Effect of λ on fluid temperature, B_r =0.3, α *=1.2*

The derived analytical solutions for the fluid temperature distributions in the half-circular coordinate system are shown numerically in Figs. 14–21, and the resulting graphics are displayed in Fig. 2-27. The temperature profiles of the whole cylindrical coordinate system of the impacts of λ, α, and Br on the fluid temperature distribution in the pipe are shown in Figs. 22–27, while the effects of λ, α, and Brinkman number, Br, on the temperature profiles are shown in the figures. The temperature profile results from Hayat et al.'s work on the study of

heat transfer in pipe flow of a Johnson-Segalman fluid [20] show some discrepancies with the thermal boundary conditions of the developed models, despite the fact that different studies have been conducted later using different techniques. This is because, as their data demonstrate, thermal boundary conditions are not met. As a result, the current work used finite difference methos to reexamine the earlier analysis and presents the findings appropriately.

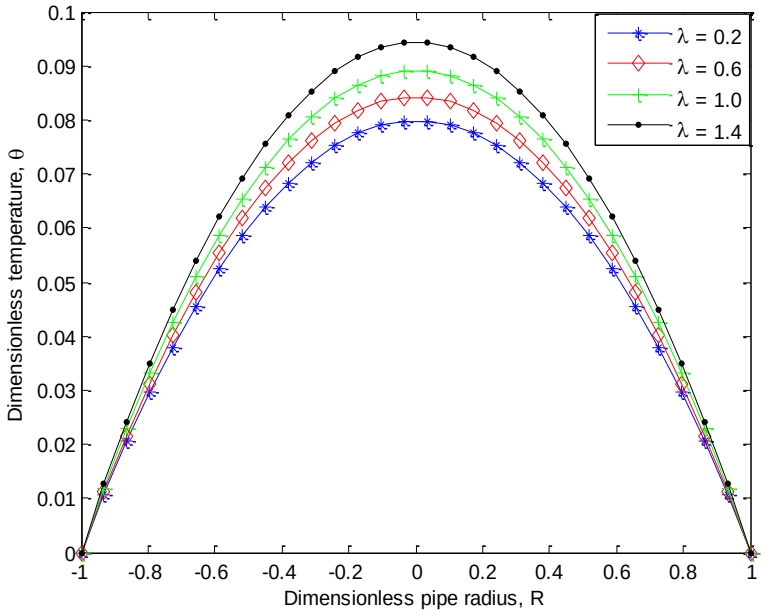

Fig. 22. Effect of λ on the fluid temperature, B_r =0.4, α =*0.5*,

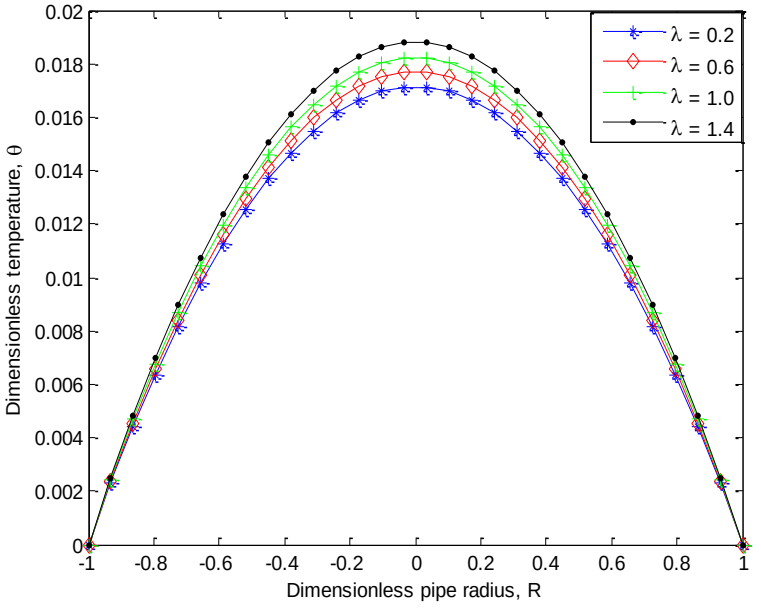

Fig. 23. Effect of λ on fluid temperature, B_r =0.4, α =*1.2*

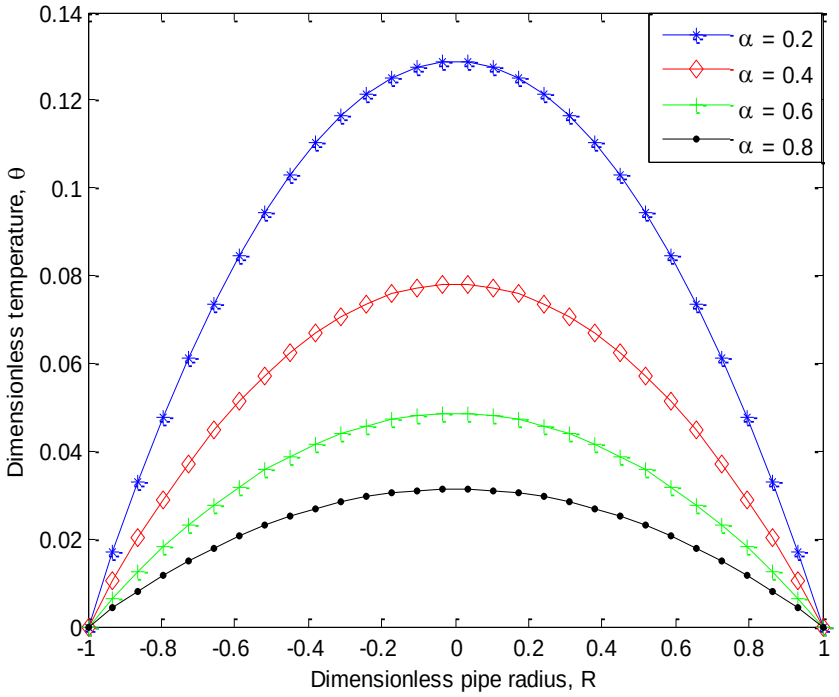

Fig. 24. Effect of α on the fluid temperature, B_r =0.2, λ =*0.5*,

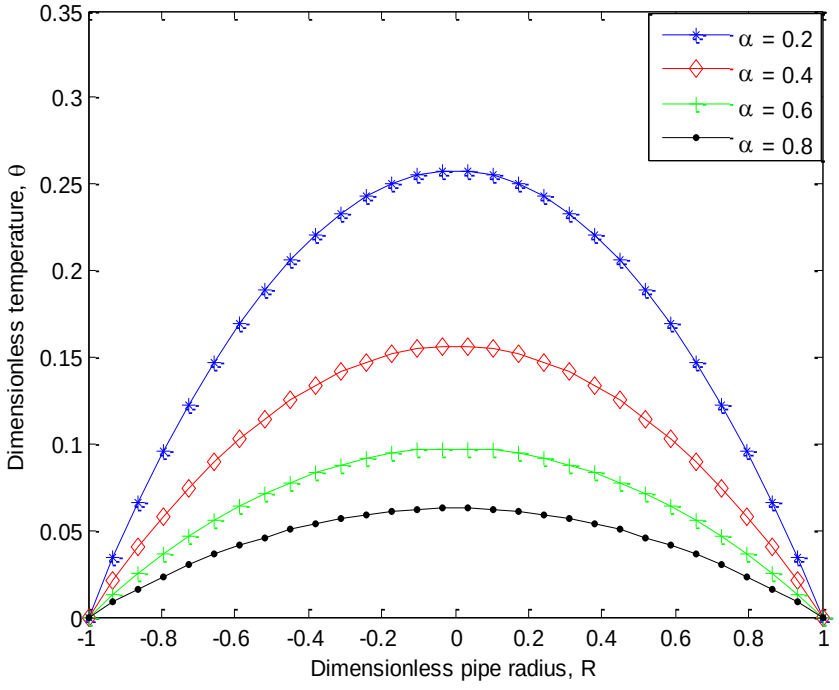

Fig. 25. Effect of α on fluid temperature, B_r =0.4, λ =*0.5*

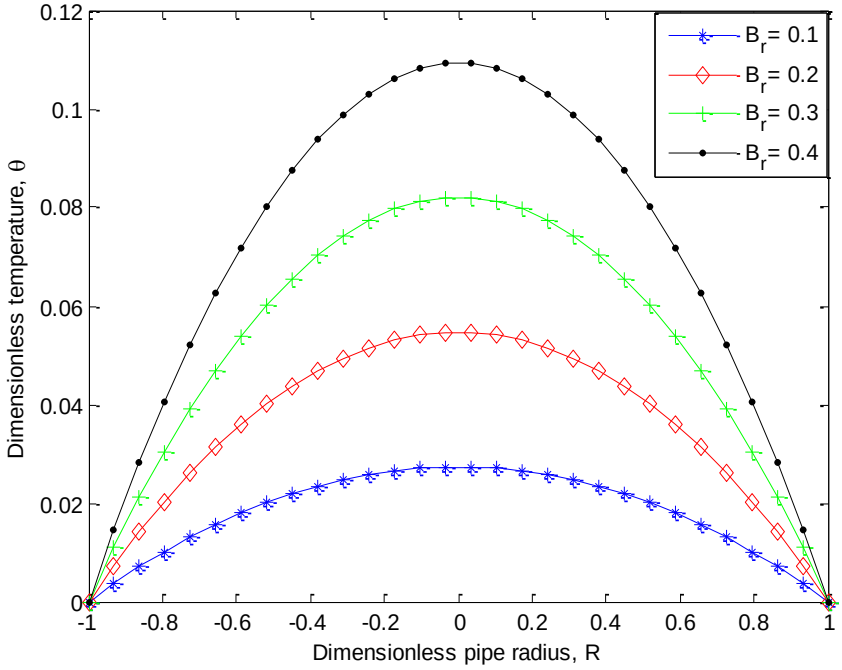

Fig. 26. Effect of B_r on the fluid temperature, α =0.5, λ =*0.5*,

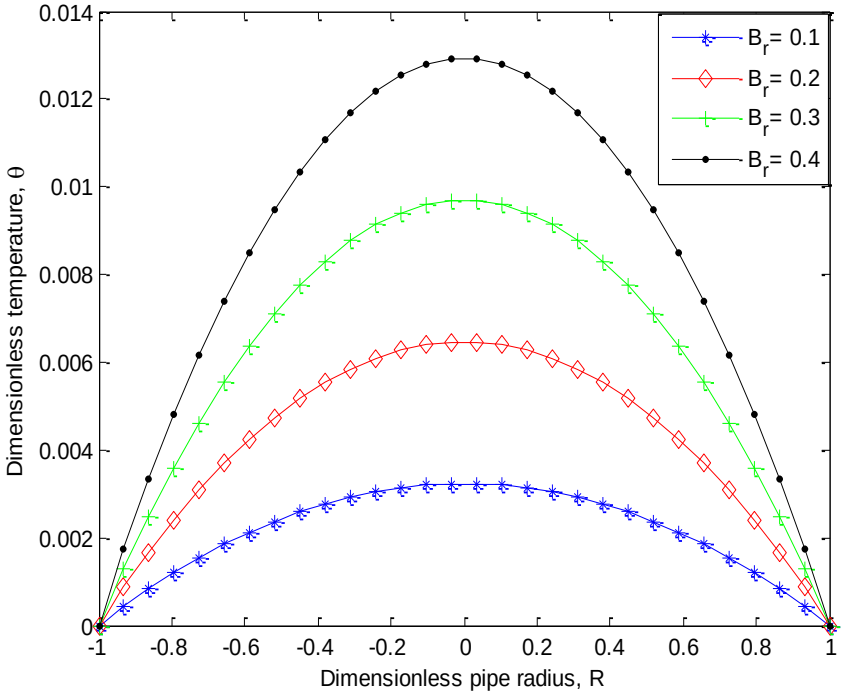

Fig. 27. Effect of B_r on fluid temperature, α =1.5, λ =*0.5*

As demonstrated in Figs. 14 and 15, it is evident from the figures that the fluid temperature rises as Br increases for various positive values of λ and α. Figures 26 and 27 depict the temperature profiles of the entire cylindrical coordinate system and show the same tendencies. The effects of α on the fluid temperature distributions for various positive values of Br and λ are shown in Figs. 16–17 and Figs. 24–25. The findings indicate that the fluid's temperature profile lowers as α rises. The increased fluid viscosity is the cause of this. Additionally, Figs. 18–23 demonstrate the effects of λ on the fluid temperature. The figures demonstrate that for various positive values of Br and α, a rise in λ results in an increase in fluid's temperature. This could be the result of the flow's relaxation time increasing.

5. CONCLUSION

This paper has applied the finite difference approach to analyze the Johnson-Segalman steady flow and heat transfer behaviors in a pipe. The results of the numerical solution demonstrate that the fluid's temperature and velocity rise as the relaxation time parameter and Brinkman number do. Additionally, it was shown that the relaxation time parameter rises as fluid velocity increases but falls as fluid temperature rises. It should be noted that as the viscosity parameter gets closer to unity and beyond unity, the effects of relaxation parameters on the velocity distribution become negligible.

Nomenclature:

a slip parameter.
c_p specific heat capacity, and
D symmetric part of the velocity gradient
k thermal conductivity,
p *fluid* pressure,
$-pI$ indeterminate part of the stress
S extra stress tensor,
t time,
T fluid temperature,
$\bar{u}$ flow velocity
W s kew symmetric part of the velocity gradient
η kinematic viscosity
μ dynamic viscosity
ξ relaxation time
ρ fluid density,
σ Cauchy stress tensor

References

[1] G. Astarita, G. Marrucci, Principles of Non-Newtonian Fluid Mechanics, McGraw-Hill, London, 1974.

[2] R.B. Bird, R.C. Armstrong, O. Hassager, Dynamics of Polymeric Liquids, Fluid Dynamics, vol. 1, Wiley, New York, 1987.

[3] X. Qiu, J. Duan, J. Luo, P. N. Kaloni , Y. Liu. Parameter effects on shear stress of Johnson–Segalman fluid in Poiseuille flow. International Journal of Non-Linear Mechanics, 55 (2010), 140–146.

[4] R.I. Tanner, Engineering Rheology, Oxford UniversityPress,Oxford,1992.

[5] M. W. Johnson, D. A. Segalman, Model for viscoelastic fluid behavior which allows non-affine deformation. J. Non Newton. Fluid Mech., 2 (1977), 255–270.

[6] M.W. Johnson, D. Segalman, A new model for viscoelastic fluid behavior which allows non-affine deformation, Journal of Non-Newtonian Fluid Mechanics, 2 (1977), 255–270

[7] I.J. Rao, K.R. Rajagopal, Some simple flows of a Johnson–Segalman fluid, Acta Mechanica, 132 (1999), 209–219.

[8] R.W. Kolkka, D.S. Malkus, M.G.Hansen, G.R.Ierley, Spurt phenomena of the Johnson–Segalman fluid and related models, Journal of Non-Newtonian Fluid Mechanics, 29 (1988), 303–335, 1988.

[9] I.E. Ireka, T. Chinyoka, Non-isothermal flow of a Johnson–Segalman liquid in a lubricated pipe with wall slip, Journal of Non-Newtonian Fluid Mechanics, 192 (2013), 20–28.

[10] S. Nadeem, N.S. Akbar, Influence of heat and mass transfer on the peristaltic flow of a Johnson–Segalman fluid in a vertical asymmetric channel with induced MHD, J. Taiwan Inst. Chem. Eng. 42 (2011), 58–66.

[11] T. Hayat, Y. Wang, A.M. Siddiqui, K. Hutter, Peristaltic motion of a Johnson–Segalman fluid in a planar channel, Math. Probl. Eng. 1 (2003), 1–23.

[12] T. Hayat, F.M. Mahomed, S. Asghar, Peristaltic flow of a magnetohydrodynamic Johnson–Segalman fluid, Nonlinear Dynam. 40 (2005), 375–385.

[13] M. Elshahed, M. Haroun, Peristaltic transport of a Johnson–Segalman fluid under effect of a magnetic field, Math. Probl. Eng., 6 (2005), 663–667.

[14] R. W. Kolkka, D.S. Malkus, M.G. Hansen, G.R. IerIy, A.R. Worthing, Spurt phenomenon of the Johnson–Segalman fluid and related models, J. Non-Newton. Fluid Mech. 29 (1988), 303–335.

[15] I. J. Rao, K.R. Rajagopal, Some simple flows of a Johnson–Segalman fluid, Acta Mech. 132 (1999), 209–219.

[16] M.K. Alam, A.M. Siddiqui , M.T. Rahim, S. Islam Thin-film flow of magnetohydrodynamic (MHD) Johnson–Segalman fluid on vertical surfaces using the Adomian decomposition method. Applied Mathematics and Computation, 219 (2012), 3956–3974.

[17] S. Hina, T. Hayat, A. Alsaedi Heat and mass transfer effects on the peristaltic flow of Johnson–Segalman fluid in a curved channel with compliant walls International Journal of Heat and Mass Transfer, 55 (2012), 3511–3521.

[18] Y. Wang, T. Hayat, K. Hutter, Peristaltic transport of a Johnson–Segalman fluid through a deformable tube, Theor. Comput. Fluid Dyn, 21 (2007), 369–380.

[19] J. Howell. Numerical approximation of shear-thinning and Johnson–Segalman viscoelastic fluid flows. A Dissertation Presented to the Graduate School of Clemson University, 2007.

[20] T. Hayat, Z. Iqbal, M. Sajid, K. Vajravelu. Heat transfer in pipe flow of a Johnson–Segalman fluid, International Communication in Heat and Mass Transfer, 35 (2008), 1297–1301.

[21] T. Hayat, R. Ellahi, S. Asghar. The influence of variable viscosity and viscous dissipation on the non-Newtonian flow: Analytical solution. Communication in Nonlinear Science and Numerical Simulation, 12 (2007), 300–313.

[22] A. Fernandez, On some approximate methods for nonlinear models. Appl Math Comput., 215 (2009) 168-74

[23] A. Aziz, and M. N. Bouaziz. A least squares method for a longitudinal fin with temperature dependent internal heat generation and thermal conductivity, Energy Conversion and Management, 52 (2011), 2876-82